Supporting Information for

Efficient Strategy of 2D ^{11}B-^{11}B Solid-State NMR Spectroscopy for Monitoring Covalent Self-Assembly of Boronic Acid-Derived Compounds: Transformation and Unique Architecture of Bortezomib Molecules in Solid State

Jiri Brus,[a*] Jiri Czernek,[a] Martina Urbanova,[a] Libor Kobera,[a] and Alexandr Jegorov[b]

[a)] Institute of Macromolecular Chemistry, Academy of Sciences of the Czech Republic, Heyrovsky sq. 2, 162 06 Prague 6, Czech Republic.
[b)] TEVA Pharmaceutics, Branisovska 31, 370 05 Ceske Budejovice, Czech Republic.

AUTHOR EMAIL ADDRESSES: brus@imc.cas.cz, czernek@imc.cas.cz, kobera@imc.cas.cz urbanova@imc.cas.cz, Alexandr.Jegorov@tevapharm.cz

Supporting Information S1 –Solid-State NMR Spectroscopy (Experimental Details)

1D MAS NMR experiments: All solid-state NMR spectra were measured at 11.7 T using a Bruker Avance 500 WB/US NMR spectrometer (2013) in a double-resonance 4-mm, 3.2-mm and 2.5-mm probe-head at spinning frequencies 11, 20 and 30 kHz, respectively. The ^{11}B MAS NMR spectra were acquired at 160.42 MHz; spinning frequency was $\omega_r/2\pi$= 20 kHz; 20° pulse width was 1 μs; recycle delay of 4 s; and the number of scans was 2048. ^{13}C CP/MAS NMR spectra employing cross-polarization were acquired using the standard pulse scheme at spinning frequency of 11 kHz. The recycle delay was 4 s and the cross-polarization contact time was ranging from 0.1 to 3 ms. The strength of spin-locking fields B_1(^{13}C) expressed in frequency units $\omega_1/2\pi$=γB_1 was 64 kHz. The spectra were referenced to α-glycine (176.03 ppm).

*2D ^{1}H-^{13}C FSLG HETCOR MAS NMR experiments:* Two-dimensional (2D) ^{1}H-^{13}C HETCOR experiments were performed using the FSLG (Frequency Switched Lee-Goldburg) decoupling during the t_1 evolution period consisting of 64-128 increments each made of 440 scans with a dwell time of 42.6 μs (**Figure S1**). Rotation frequency was $\omega_r/2\pi$ = 11 kHz. The B_1(^{1}H) field strength of FSLG and SPINAL-64 decoupling expressed in frequency units $\omega_1/2\pi$=γB_1 was 89.3 kHz.
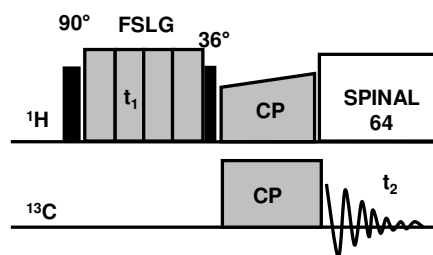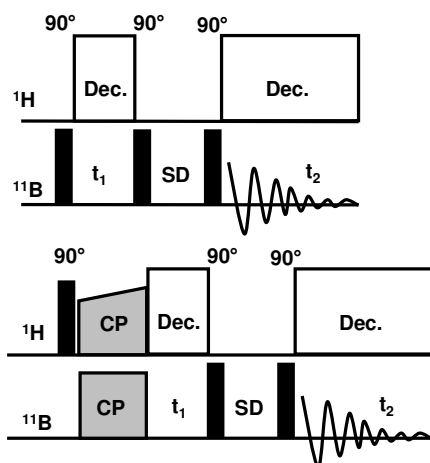

Figure S1. Schematic representation of 2D ^{1}H-^{13}C FSLG HETCOR MAS NMR experiment.

^{11}B TQ/MAS NMR: The 2D triple-quantum (TQ) ^{11}B TQ/MAS NMR spectra were measured using the three-pulse sequence with the excitation, reconversion and selective pulses of 4.2, 1.5 and 43 μs lengths,

respectively. The reconversion and selective pulses were spaced by the *z*-filter of 20 μs length (**Figure S2**). The dipolar decoupling SPINAL 64 was applied during both detection periods.
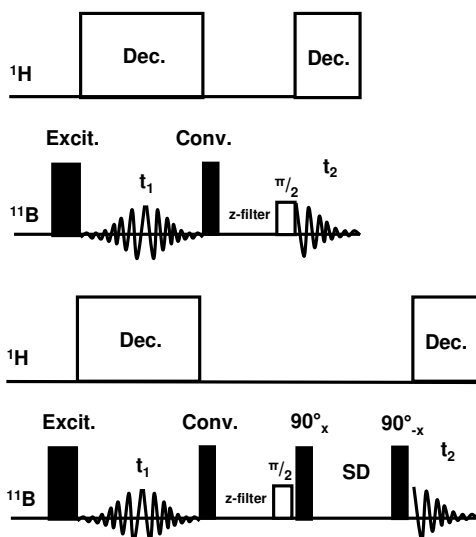
Figure S2. Schematic representation of 2D ^{11}B TQ/MAS NMR experiment (up) and modified 2D ^{11}B TQ/MAS NMR experiment with a spin-diffusion period (bottom).


Figure S3. Schematic representations of 2D ^{11}B-^{11}B PDSD NMR experiments: a three-pulse NOESY-type experiment with direct excitation of [11]B magnetization (up); a PDSD experiment employing [1]H-[11]B cross polarization (bottom).

^{11}B-^{11}B PDSD MAS NMR: The 2D ^{11}B-^{11}B MAS NMR correlation spectra were measured using two different experimental arrangements. Primarily, the standard three-pulse (NOESY-type) pulse sequence (**Figure S3 up**) was applied. Alternatively, the proton-driven spin diffusion (PDSD) experiment employing [1]H-[11]B cross-polarization instead of the single-pulse excitation was applied (**Figure S3 bottom**). In both cases spinning frequency of $\omega_r/2\pi = 11$ kHz was used; the recycle delay was 4 s and the cross-polarization contact time was 0.1 ms. In both cases the t_1 evolution period consisted of 128 increments each made of 256 scans; the spin-diffusion period varied from 0.1 to 300 ms; and the dipolar decoupling SPINAL 64 was applied during both detection periods.

^{11}B-^{11}B PDSD TQ/MAS NMR: The 2D ^{11}B-^{11}B PDSD TQ/MAS NMR experiments with the excitation and indirect detection of triple-quantum [11]B coherence were measured using the pulse sequence demonstrated in **Figure S2 (bottom)**. The spin-diffusion period spaced by two hard 90 degree pulses.

^{11}B-^{11}B DQ/SQ MAS NMR correlation experiments: The 2D ^{11}B-^{11}B DQ/SQ MAS NMR correlation spectra were measured using the [11]B-[11]B double-quantum (DQ) experiment employing the BR2$^1_2$ recoupling sequence at spinning frequency $\omega_r/2\pi = 20$ kHz (**Figure S4**). The recycle delay was 4 s, t_1 evolution period consisted of 64-128 increments each made of 512 scans. The DQ coherence excitation and reconversion consisted of 1-25 loops (duration of one loop was 200 μs). The dipolar decoupling SPINAL 64 was applied during both detection periods and LG-cw decoupling was used during the build-up of DQ coherence. Fast-amplitude modulation sequence (FAM) consisting of 2 loops was used for [11]B signal enhancement.
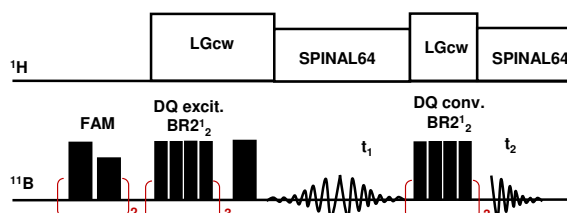
Figure S4. Representation of 2D [11]B-[11]B DQ-SQ experiment with FAM excitation and BR2$^1_2$ recoupling sequence.

Supporting Information S2 – Validation of of 2D ^{11}B-^{11}B MAS NMR Spin-Exchange Correlation Experiments

To identify medium-range interatomic distances between the boron atoms that are expected in boroxine moiety (ca. 2.6 Å) three types of complementary 2D [11]B-[11]B correlation experiments employing single- and/or double-quantum [11]B coherence transfer as described above were tested using the following model compounds:

i) borax (disodium tetraborate, $Na_2[B_4O_5(OH)_4] \cdot 8H_2O$)
ii) cesium cobalt(3) bis(dicarbollide) clusters (CsCoD)
iii) boric acid (BH_3O_3)
iv) (2-Methylpropyl)boronic acid (($CH_3)_2CHCH_2B(OH)_2$)
i) [(E)-4-(2-Cyano-2-ethoxycarbonylvinyl)phenyl] boronic acid pinacol ester ($C_{18}H_{22}BNO_4$)

These crystalline compounds represent typical examples in which different boron-boron interatomic distances can be found. Crystalline borax represents a molecular system in which medium-range boron-boron distances of ca. 2.6 Å dominate. These interatomic distances are defined by the covalent bonds and valence angle in B-O-B structural motifs. Crystalline cesium cobalt(3) bis(dicarbollide) (CsCoD) then represents a boron-rich system in which short-range one-bond boron-boron spin pairs separated by ca. 1.7 Å dominate. In contrast, crystalline boric acid is a suitable example of the molecular system in which boron atoms are not directly coupled by covalent chemical bonds, intermolecular interactions are provided by hydrogen bonding B-O….H-O-B allowing thus formation of long-range boron-boron spin pairs.

Moreover, crystalline boric acid consists of layers of $B(OH)_3$ molecules held together by these hydrogen bonds. The B-O bond length is 136 pm and the O-H is 97 pm with a hydrogen bond of 272 pm. The distance between two adjacent layers is 318 pm. Consequently, typical boron-boron interatomic distances in crystalline boric acid reach of ca. 3.6 Å. A bit larger boron-boron interatomic distances (>4 Å) caused by the presence of a relatively small hydrophobic substituent can be expected in crystalline 2-methyl-propyl-boronic acid. A compound [(E)-4-(2-Cyano-2-ethoxycarbonylvinyl)-phenyl]boronic acid pinacol ester ($C_{18}H_{22}BNO_4$) then represents the model system in which basically isolated boron atoms with a distance larger than 5 Å are expected.

### ad. i) 2D [11]B-[11]B Correlation Experiments on Borax

Borax crystallizes in the monoclinic system with B2/b space group and unit cell parameters a = 12.0012(2) Å, b = 10.644 Å, c = 11.879 Å and β = 106.617(1)° (**Figure S5**).[1] Due to the well-defined crystal structure and the presence of two chemically distinct boron sites (B[III] and B[IV]) that are covalently bound through an oxygen atom, crystalline borax represents the most suitable model for searching the boroxine motifs. In particular, the bi-cyclic borax molecule, in which boron atoms adopting different local geometry are separated by 2.5 Å (B[III]-B[IV], intramolecular) and 3.6 Å (B[III]-B[III], intramolecular, **Figure S5**), offers a perfect model to probe evolution of ^{11}B-^{11}B spin-exchange NMR correlation signals that can be expected also in the boroxine structure units.
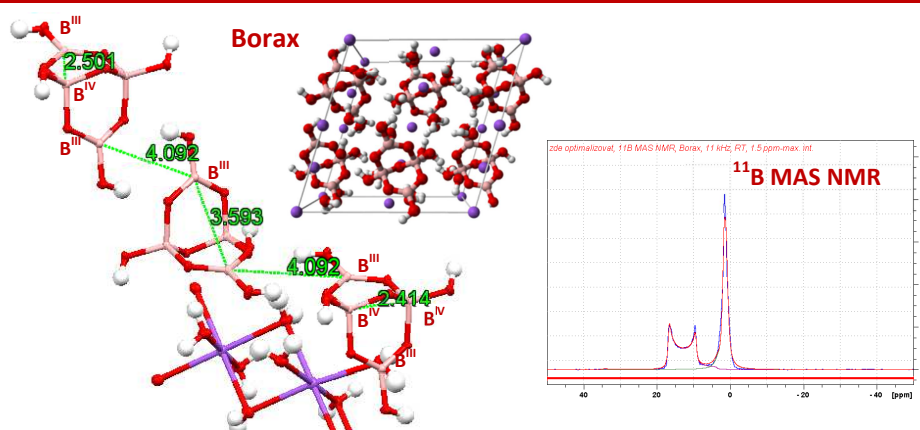

Figure S5 Crystal structure of borax adopted from [**ref. 1**] and the corresponding ^{11}B MAS NMR spectrum with a line-shape simulation (isotropic chemical shift δ([11]B) = 19.0 and 2.1 ppm; second-order quadrupolar splitting Q_{cc} = 2.5 and 0.9 MHz; asymmetry parameter of η = 0.03 and 0.0).

^{11}B-^{11}B PDSD MAS NMR: At 20-25 kHz in 3.2 mm probe-head using the standard 2D ^{11}B-^{11}B three-pulse NOESY-type PDSD MAS NMR sequence with ^{1}H decoupling during both evolution periods the off-diagonal signals correlating the chemically non-equivalent B^{III} and B^{IV} atoms separated by a distance of ca. 2.5 Å are fully developed within ca. 100 ms mixing (**Figures S6 and S7**).

a)   b)
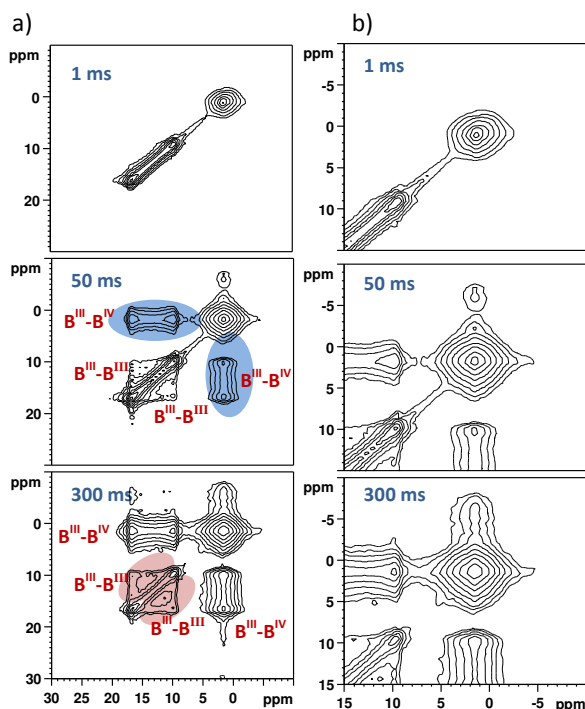
Figure S6. Full-range ^{11}B-^{11}B PDSD NMR correlation spectra of borax (a); and expanded regions of B^{IV} sites (b) measured with ^{11}B-^{11}B spin-diffusion mixing times of 1, 50 and 300 ms.

In contrast, the *autocorrelation* off-diagonal signals B^{III}-B^{III} representing the spin-exchange between the chemically equivalent but magnetically non-equivalent B^{III} boron sites separated by 3.6 Å are not completely evolved even within 300 ms. It is worthy to note that these off-diagonal signals also considerably broaden at longer mixing times. As demonstrated below this broadening as well as the evolution of these autocorrelation signals can substantially decrease spectral resolution in the correlation ^{11}B-^{11}B PDSD MAS NMR spectra measured at long mixing times. This is particularly critical for the spectra overcrowded by a range of different coherences with an extensive signal overlap.
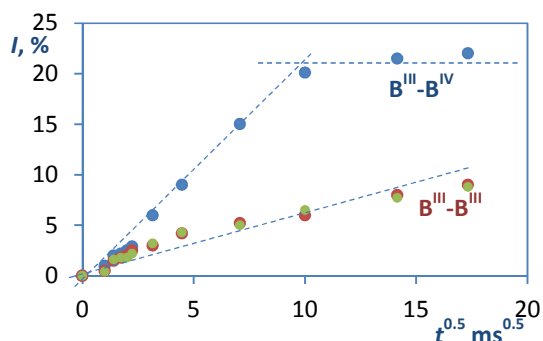
Figure S7. ^{11}B-^{11}B spin-diffusion build-up curves reconstructed for off-diagonal correlation signal B^{III}-B^{IV} and auto-correlation signal B^{III}-B^{III}.

2D ^{11}B-^{11}B TQ/MAS PDSD NMR: The modified ^{11}B TQ/MAS PDSD NMR experiment represents a promising opportunity to enhance spectral resolution. By incorporating the spin-exchange period after the reconversion of TQ coherence, and by the switching off the ^{1}H decoupling (**Figure S2**) the ^{11}B-^{11}B spin exchange is launched and the correlation signals can effectively evolve. By selecting the triple-quantum coherence and by applying the appropriate spectral transformation the resolution of recorded ^{11}B-^{11}B correlation spectra can be substantially increased.

In the case of crystalline borax the relatively well-evolved correlation signals were detected in the 2D ^{11}B-^{11}B TQ/MAS PDSD NMR spectra employing the 100 ms spin-diffusion mixing time. Moreover, no *autocorrelation* signals indicating polarization transfer between the magnetically non-equivalent B^{III} boron sites evolved (**Figure S6**). Comparing the different processing of the recorded ^{11}B TQ/MAS PDSD NMR spectra, the unprocessed (unsheared) correlation spectrum provided basically the typical correlation pattern (**Figure S6**). On the other hand, this experiment is significantly less-sensitive in comparison with the NOESY-type ^{11}B-^{11}B PDSD MAS NMR technique.

4
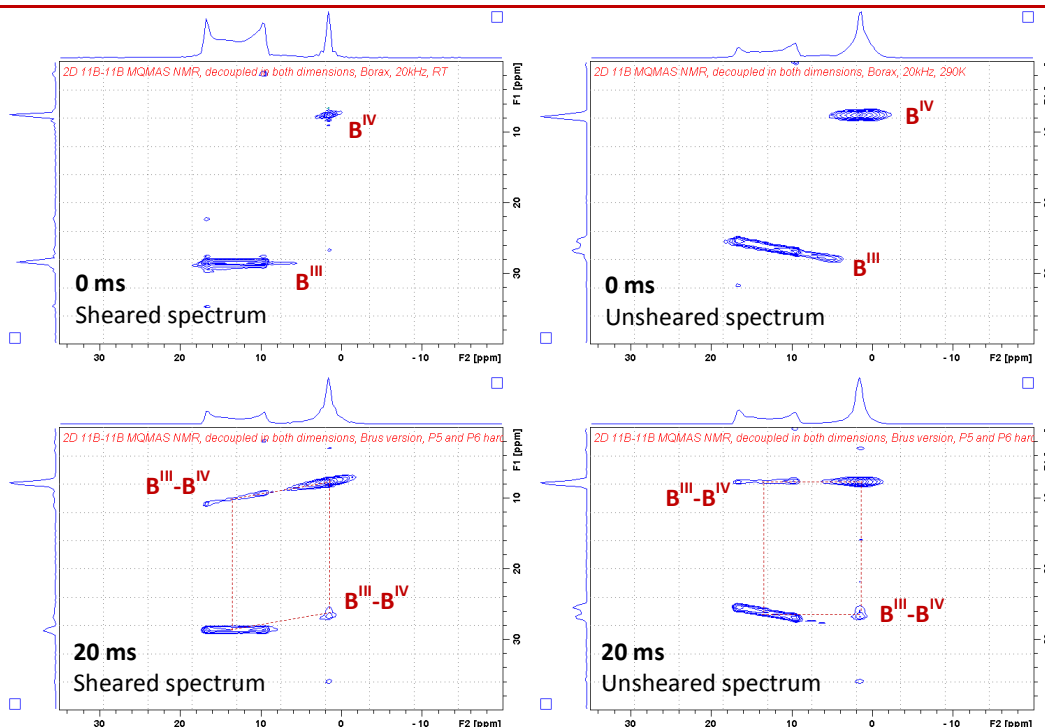
Figure S8. ^{11}B-^{11}B TQ/MAS PDSD NMR correlation spectra of borax measured with [11]B-[11]B spin-diffusion mixing times 0 and 20 ms (upper and lower row, respectively).

2D ^{11}B-^{11}B DQ/SQ BR2$^1_2$ MAS NMR of borax: To obtain an alternative view onto boron-boron correlations, we utilized the recently developed 2D ^{11}B-^{11}B DQ/SQ BR2$^1_2$ NMR correlation technique that, in contrast to 2D ^{11}B-^{11}B PDSD, suppresses the relayed spin-diffusion transfer and allows for the evolution of autocorrelation signals only if the chemically and magnetically equivalent nuclei are spatially close and mutually interact through the dipolar couplings. In other words, the diagonal signals of isolated non-interacting boron species cannot evolve. As demonstrated in **Figure S9** at 20 kHz in 3.2 mm probe-head the efficient excitation of ^{11}B-^{11}B double-quantum (DQ) coherence required application of ca. 2-5 recoupling loops (length of a single recoupling loop is 200 µs). The fully in-phase DQ-filtered signals were generated using at least 2-3 recoupling cycles. The application of 1 recoupling cycle lead to the distorted (partially dispersed) DQ-filtered signal that was *contaminated* by incompletely suppressed single-quantum coherences. However, bearing in mind that that the purpose of this testing is finding the conditions for identification of medium-range ^{11}B-^{11}B spin pairs (ca. 2.5 Å), we recorded the 2D ^{11}B-^{11}B DQ/SQ BR2$^1_2$ NMR correlation spectra for the whole range of recoupling cycles starting from 1 to 10 covering thus recoupling times 200-2000 µs. The most typical examples of the obtained spectra are demonstrated in **Figure S9**.
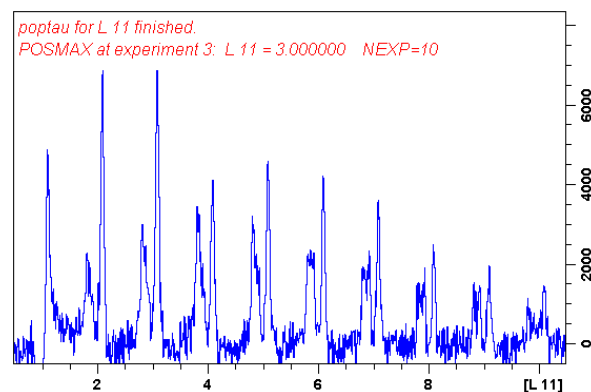
Figure S9. Optimization of ^{11}B-^{11}B DQ/SQ BR2$^1_2$ MAS NMR sequence performed on borax. Number of recoupling loops was optimized. Length of the recoupling loop was 200 µs (synchronized with MAS frequency).

5
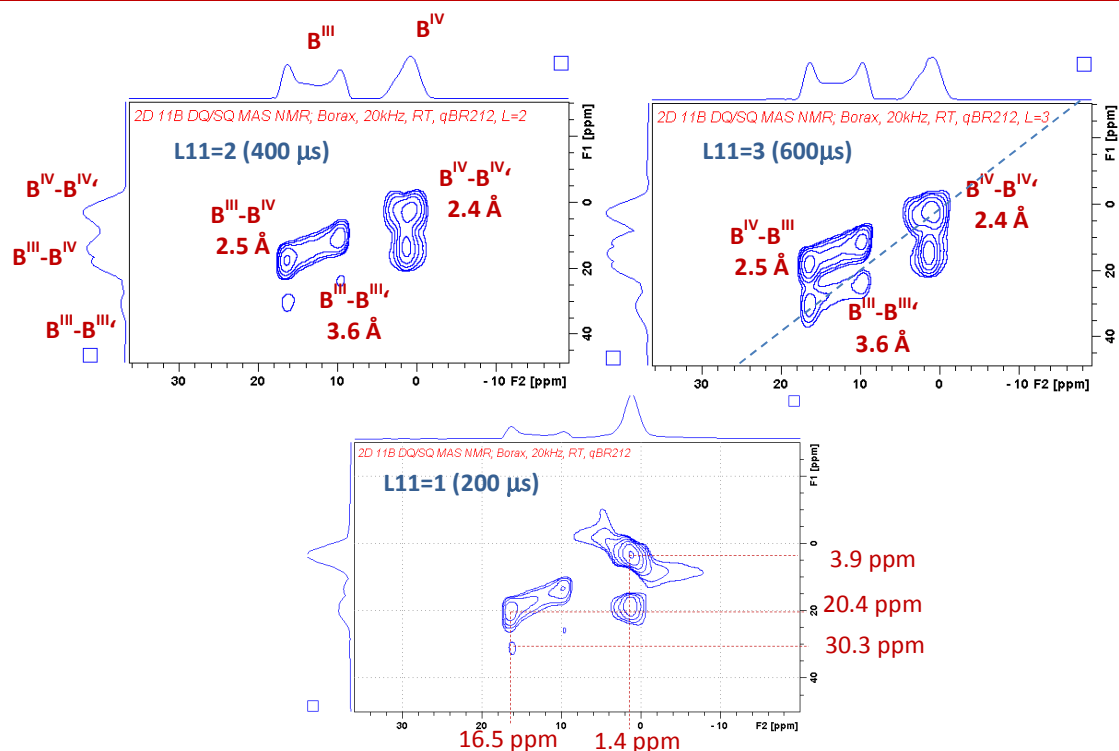
Figure S10. 2D ^{11}B-^{11}B DQ/SQ BR2$^1_2$ MAS NMR spectra of borax measured at 400, 600 and 200 µs recoupling times.

As demonstrated in **Figure S10** the medium-range hetero-correlation signals B^{III}-B^{IV} as well as the autocorrelation signals B^{IV}-B^{IV} reflecting the interatomic distances of ca. 2.5 Å are clearly apparent even in the spectrum measured with the 400 µs recoupling period (2 cycles). In contrast, the long-range autocorrelation signal B^{III}-B^{III} reflecting ca. 3.6 Å spin pairs is still very weak. By applying the 600 µs recoupling period (3 cycles), however, this long-range signal is well evolved, and reaches maximum intensity at ca. 800-1200 µs. As expected the correlation signals detected in the 2D ^{11}B-^{11}B DQ/SQ BR2$^1_2$ MAS NMR spectrum measured with the shortest possible recoupling period (1 recoupling cycle) exhibit presence of a dispersive spectral mod. These wings of B^{IV}-B^{IV} correlation signals are clearly apparent. However, bearing in mind the isotropic chemical shifts of boron sites B^{III} and B^{IV} $\delta(^{11}B)$= 19.0 and 2.5 ppm, respectively, the detected correlation signals still give the expected double-quantum frequencies although the intensities of these signals are relatively low. It is worthy to note that the long-range autocorrelation signal B^{III}-B^{III} is nearly below the detection limit.

ad. ii) 2D ^{11}B-^{11}B experiments on cesium cobalt(3) bis(dicarbollide) clusters (CsCoD)

In contrast to the crystalline borax with its typical medium-range B-O-B interatomic distances, crystalline cesium cobalt(3) bis(dicarbollide) clusters (CsCoD) represent a boron-rich molecular system in which short-range intramolecular ^{11}B…^{11}B distances of ca. 1.7-1.8 Å predominate (**Figure S11**).
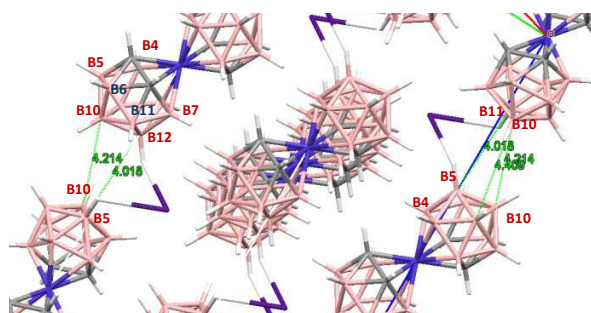

**Figure S11**. Packing of CoD ions in the crystalline CsCoD adopted from [**ref. 2**].

6

Moreover, due to the presence of 9 structurally non-equivalent boron atoms in the dicarbollide clusters the resulting ^{11}B MAS NMR spectra are overcrowded by a number of strongly overlapped signals. Consequently, this molecular system represents a unique crystalline model for probing the spectral resolution of various [11]B-[11]B correlation experiments. It is worthy to note, however, that relatively small quadrupolar second-order splitting of all boron sites of dicarbollide clusters makes the interpretation of the detected 2D correlation spectra still relatively straightforward.

^{11}B-^{11}B PDSD MAS NMR: At 20-25 kHz in 3.2 mm probehead using the standard 2D [11]B-[11]B three-pulse NOESY-type PDSD sequence with ^{1}H decoupling applied during both evolution periods the off-diagonal signals correlating the directly bonded [11]B atoms separated by a distance of ca. 1.7-1.8 Å are fully developed within the 10 ms mixing period (**Figure S12**). However, the first indication of such a short-range correlation is reflected by weak off-diagonal signals evolved within 0.1 ms. This fact indicates that [11]B-[11]B spin exchange in the protonated systems is a fairly efficient process that can basically provide direct structural data.

Correlation signals indicating medium-range correlations between the boron atoms separated by ca. 2.9 Å are apparent in the 2D spectra measured with the mixing period of ca. 10 ms and longer. At these relatively long mixing times two negative phenomena were observed. At first and as already mentioned above, the spectral resolution decreases as a result of evolution of autocorrelation signals. This is clearly apparent for B6 and B11,5 signals the splitting of which nearly disappeared at longer mixing times. At second, overall intensity of the recorded spectra considerably decreased at longer mixing times. Nevertheless, there is still a good chance to record the 2D ^{11}B-^{11}B PDSD NMR correlation spectrum of protonated organic compound in which the long-range correlation signals will be detected.
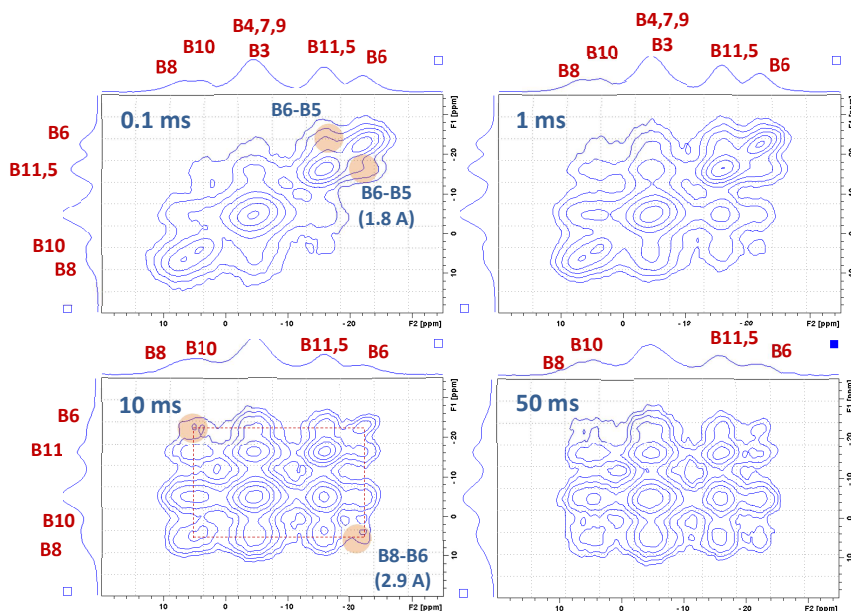
Figure S12. ^{11}B-^{11}B PDSD NMR spectra of CsCoD measured with [11]B-[11]B spin-diffusion mixing times of 0.1; 1; 10 and 50 ms.
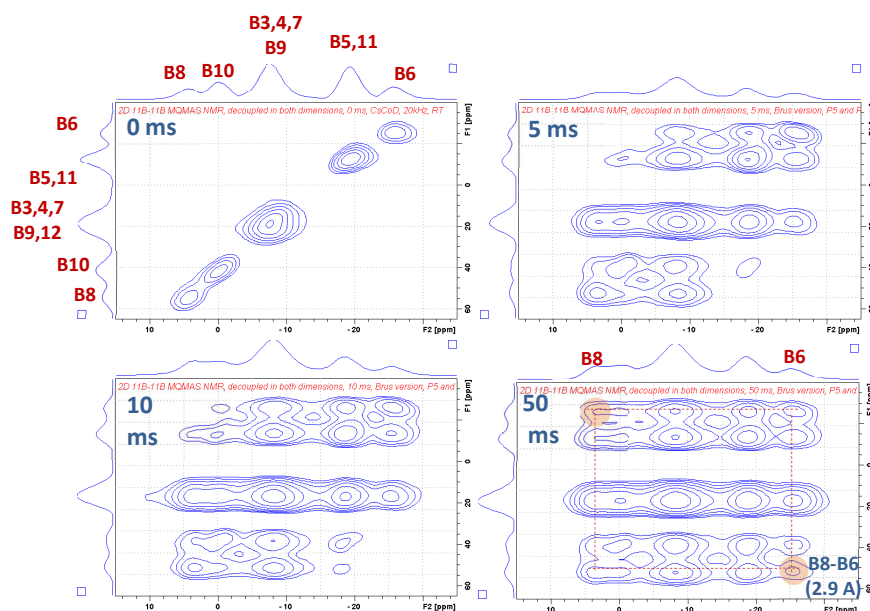
Figure S13. ^{11}B-^{11}B TQ/MAS PDSD NMR spectra of CsCoD measured with ^{11}B-^{11}B spin-diffusion mixing times 0, 5, 20 and 50 ms.

2D ^{11}B-^{11}B TQ/MAS PDSD NMR: To enhance spectral resolution of the ^{11}B-^{11}B PDSD MAS NMR correlation spectra measured at long mixing time we again applied the modified ^{11}B-^{11}B TQ/MAS PDSD NMR experiment employing the variable spin-exchange period (**Figure S2**). From the obtained unsheared ^{11}B-^{11}B TQ/MAS PDSD NMR spectra demonstrated in **Figure S13** it is clear that detection of TQ coherence in the F_1 dimension enhanced spectral resolution in such a way that the long-range correlation signal B8-B6 is perfectly separated. It worthy to note, that this correlation signal in the standard NOESY-type ^{11}B-^{11}B PDSD NMR spectrum strongly overlaps with the correlation signal B10-B6 and is barely detectable.

2D ^{11}B-^{11}B DQ/SQ BR2$^1_2$ MAS NMR of CsCoD: As demonstrated in **Figure S14** due to the short-range boron-boron interatomic distances that predominate in dicarbollide clusters the efficient excitation of ^{11}B-^{11}B double-quantum (DQ) coherence is reached even by applying the shortest DQ recoupling period (200 µs, 1 recoupling loop). Moreover, the recorded DQ-filtered signals are fully evolved without any dispersive modes. Subsequently, however, with increasing duration of recoupling periods the signals intensities rapidly decrease and fall nearly to zero at recoupling times of ca. 1000 µs. However, for probing the medium- or long-range ^{11}B-^{11}B distances it is necessary to measure the 2D ^{11}B-^{11}B DQ/SQ BR2$^1_2$ NMR correlation spectra employing the recoupling period reaching at least 600 µs. Although the intensities of DQ-filtered signals of dicarbollide clusters at this recoupling period are relatively low (ca. 25% of the maximum intensity of DQF signal) the 2D ^{11}B-^{11}B DQ/SQ BR2$^1_2$ NMR correlation spectrum can be recorded within an acceptable experimental time ca. 16-20 hours.
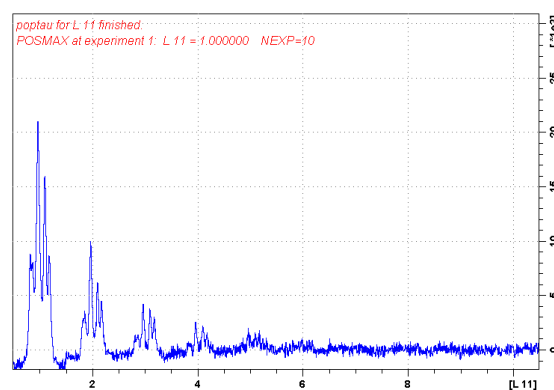
Figure S14. Optimization of ^{11}B-^{11}B DQ/SQ BR2$^1_2$ MAS NMR sequence using CsCoD. Number of recoupling loops was optimized and the length of a recoupling loop (synchronized with MAS frequency) was 200 µs.

As a result of the efficient excitation of short-range ^{11}B-^{11}B DQ coherences the 2D ^{11}B-^{11}B DQ/SQ BR2$^1_2$ MAS

8

NMR spectrum of CsCoD measured at 200 μs is dominated by the signals reflecting one-bond ^{11}B-^{11}B spin pairs (**Figure S15, up**). It is worthy to note that the recorded correlations signals are fully evolved without any dispersive mode or other distortions and artifacts. With increasing length of the recoupling period to 600 μs additional correlation signals reflecting the medium-range spin pairs appear. Similarly as in the case of ^{11}B-^{11}B TQ/MAS PDSD NMR correlation experiment the B8-B6 correlation pair was detected (**Figure S15, bottom**). This finding indicates that the medium-range correlation signals corresponding to the interatomic distance of ca. 2.9-3.1 Å can be effectively detected in 2D ^{11}B-^{11}B DQ/SQ BR2$^{1}_{2}$ MAS NMR spectra also for the multiplespin systems in which strong one-bond ^{11}B-^{11}B dipolar couplings dominate.
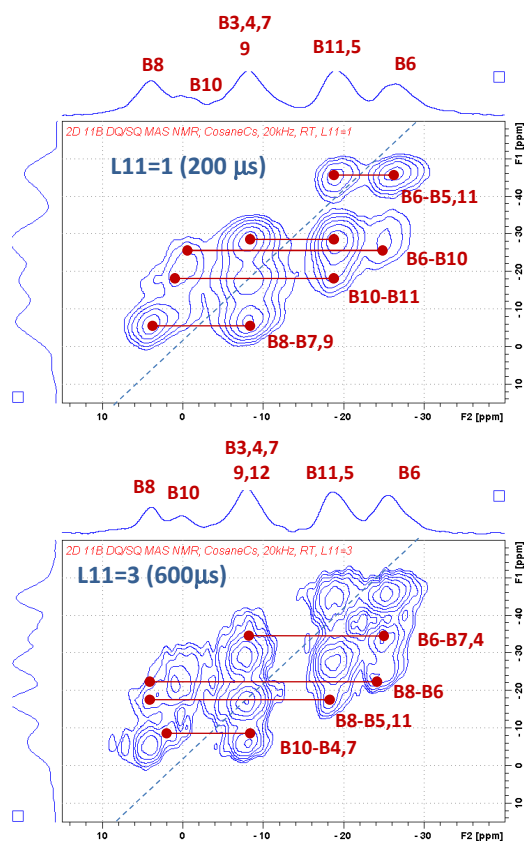

Figure S15. 2D ^{11}B-^{11}B DQ/SQ BR2$^{1}_{2}$ MAS NMR spectra of CsCoD measured at 200 and 600 μs recoupling times.

ad. iii) 2D ^{11}B-^{11}B experiments on boric acid (H$_3$BO$_3$)

In contrast to the previously discussed molecular systems in which boron atoms were directly connected by one or two chemical bonds (B-B and/or B-O-B with ca. 1.8 and 2.5 Å, respectively), the crystalline boric acid is a suitable example of the molecular system in which boron atoms form a dense network of strong hydrogen bonds.
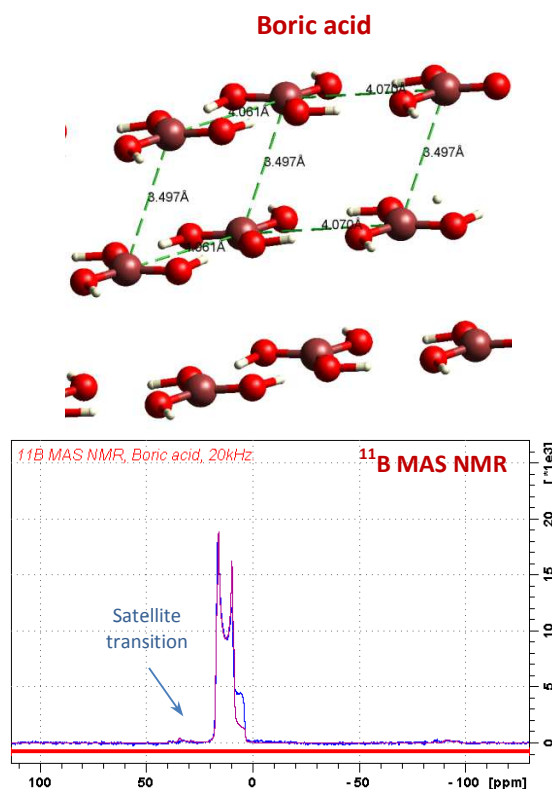

Figure S16. Crystal structure of H$_3$BO$_3$ molecules [**ref. 3**] and the corresponding ^{11}B MAS NMR spectrum with a line-shape simulation (isotropic chemical shift $\delta(^{11}$B) = 19.1 ppm; second-order quadrupolar splitting Q_{cc} = 2.5 MHz; asymmetry parameter of η = 0.16).

The intermolecular interactions in crystalline boric acid are provided by B-O….H-O-B hydrogen bonds resulting in the formation of long-range boron-boron spin pairs. Due to the layered crystal structure of boric acid (**Figure S16, up**), the typical boron-boron interatomic distances involving two layers are of ca. 3.6 Å, while 4.1 Å between the molecules located in the same layer. The crystalline boric acid also represents the spin system that is characterized by a single ^{11}B NMR signal with isotropic chemical shift $\delta(^{11}$B) = 19.1 ppm. This signal is broadened by the second-order quadrupolar splitting reaching ca. 2.5 MHz with an asymmetry parameter of η = 0.16 (**Figure S16, bottom**).

Although exploring the evolution of long-range boron-boron *autocorrealtion* signals was essential for the tracing of boroxine moieties, the spin-lattice relaxation of [11]B spins in crystalline boric acid was very slow and the complete thermal equilibrium was reached within 40 s. Consequently, only a limited number of 2D correlation experiments was recorded.

2D ^{11}B-^{11}B PDSD MAS NMR: In contrast to the crystalline borax, for which the 2D ^{11}B-^{11}B PDSD MAS NMR spectra displayed well-evolved *autocorrelation* pattern for chemically equivalent B[III]…B[III] sites separated by ca. 3.6 Å (**Figure S6**), much weaker magnetization transfer was observed for the crystalline boric acid (**Figure S17**), although the interatomic distances between the boron species are comparable.
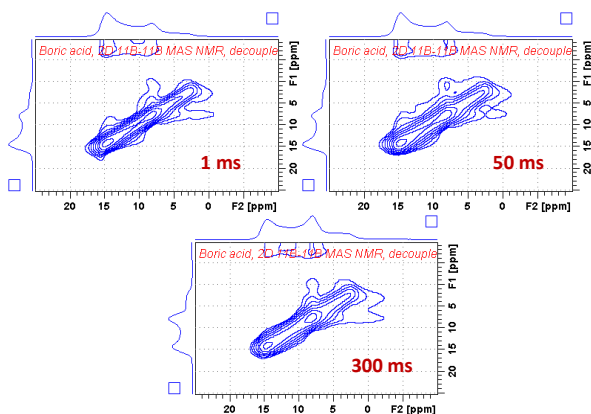
Figure S17. ^{11}B-^{11}B PDSD NMR correlation spectra of crystalline boric acid measured with [11]B-[11]B spin-diffusion mixing times of 1, 50 and 300 ms.

This difference between the [11]B spin exchange observed in crystalline borax and boric acid is given by different relative orientations of quadrupolar tensors of the interacting sites (**Figure S18**) [ref 4]. The B[III] sites in borax molecule adopt quite different relative orientations with respect to the direction of static magnetic field. Similarly the orientations of principal axes of quadrupolar tensors ($V_3 = V_{zz}$, $V_2 = V_{yy}$ and $V_1 = V_{xx}$) of these sites considerably differ. Consequently these B[III] sites are magnetically inequivalent, and thus the [11]B magnetization transfer between the individual components of the quadrupolarly broadened signal can be detected as the off-diagonal correlation signals. The mechanism of this anisotropy-driven polarization

transfer (recoupling) has been comprehensively described by *Frydman et al.* [**ref. 4**].
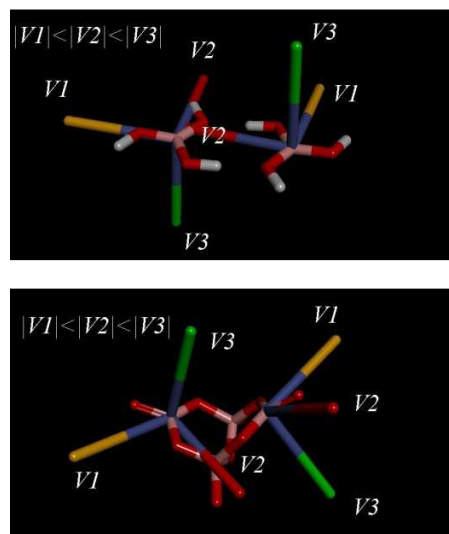

Figure S18. Crystal structure of H_3BO_3 (up) and borax (bottom) together with orientations of principal axes of quadropolar tensors.

In crystalline boric acid, however, the shortest boron-boron spin pairs are formed by the structurally identical molecules that are aligned parallel in the two neighboring layers. Consequently, the orientations of principal axes of quadrupolar tensors of the corresponding boron atoms are also quite identical making the anisotropy-driven mechanism of polarization transfer inefficient.

In contrast, as demonstrated in **Figure S18 up,** neighboring boric acid molecules, lying in the same molecular layer, exhibit slightly different relative orientations of quadrupolar tensors with respect to the static magnetic field. Specifically, the V_3 components are not parallel and the angle between these V_3 vectors is ca. 4°. Consequently, we can suppose slight magnetic nonequivalence of these sites resulting in the evolution of weak correlation signals involving the low-frequency resonances 0-5 ppm (**Figure S17**).

2D [11]B-^{11}B DQ/SQ BR2$_2^1$ MAS NMR: The build-up of [11]B DQ coherence (DQC) in crystalline boric acid demonstrated in **Figure S19** is considerably slower when compared with the DQC evolution observed for crystalline borax and CsCoD systems. This fact clearly reflects relatively long interatomic distances in the prevailing [11]B-[11]B spin pairs (3.5 and 4.1 Å). It is also

clear that the maximum intensity of DQ coherence is reached by applying a relatively long recoupling period ca. 1200-1400 μs (6-7 recoupling cycles) and nearly 80% of the maximum intensity of DQC was reached using the 600 μs recoupling period (3 cycles). In this regards, it is also worthy to note that the shortest recoupling period applied (200 μs, 1 cycle) resulted in the spectrum in which an artificial negative signal appeared. Nevertheless the corresponding 2D ^{11}B-^{11}B DQ/SQ BR2$^1_2$ MAS NMR spectrum contains the correlation signal (weak in its intensity) that is placed at expected correct SQ and DQ frequency positions (**Figure S20**).
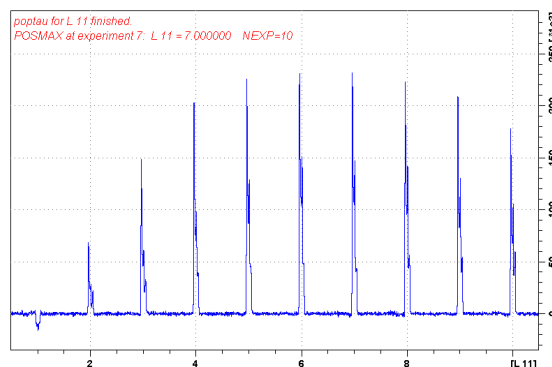
Figure S19. Optimization of ^{11}B-^{11}B DQ/SQ BR2$^1_2$ MAS NMR sequence using the crystalline boric acid. Number of recoupling loops was optimized and the length of a recoupling loop (synchronized with MAS frequency) was 200 μs.
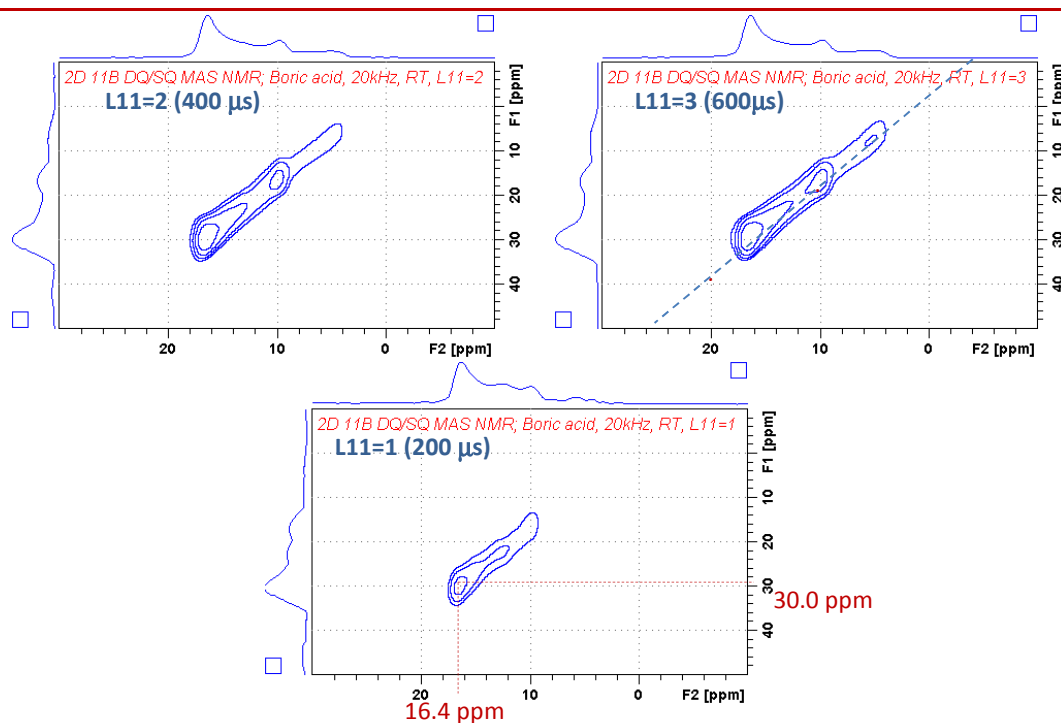
**Figure S20**. 2D ^{11}B-^{11}B DQ/SQ BR2$^1_2$ MAS NMR spectra of crystalline boric acid measured at 200, 400 and 600 μs recoupling times.

***ad. iv*) 2D ^{11}B-^{11}B experiments on (2-methylpropyl)-boronic acid ((CH_3)$_2$CHCH_2B(OH)$_2$)**

Although we do not know precise structure of crystalline (2-methylpropyl)boronic acid (MPBA) we suppose slightly longer typical boron-boron interatomic distances in this system, caused by the presence of hydrophobic 2-methylpropyl substituent. Similarly as in the case of boric acid, also the crystalline (2-methylpropyl)boronic acid represents a ^{11}B spin system which is characterized by a single ^{11}B NMR signal broadened by the second-order quadrupolar splitting.

11

The isotropic chemical shift $\delta(^{11}B)$ is 33 ppm, Q_{cc} = 3.1 MHz and asymmetry parameter i η=0.44 (**Figure S21**).
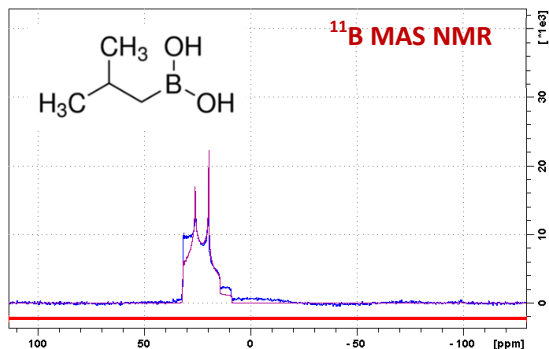

Figure S21. Chemical structure of (2-methylpropyl)boronic acid and the corresponding ^{11}B MAS NMR spectrum with a line-shape simulation (isotropic chemical shift $\delta(^{11}B)$ = 33 ppm; second-order quadrupolar splitting Q_{cc} = 3.1 MHz; asymmetry parameter of η=0.44).

2D ^{11}B-^{11}B PDSD MAS NMR: Polarization transfer in crystalline (2-methylpropyl)boronic acid during the ^{11}B-^{11}B PDSD NMR experimentation is comparable with the magnetization transfer observed in crystalline boric acid. With the increasing mixing time we observed formation of a weak correlation pattern. At 50 ms the off-diagonal signals are barely detectable. However, at 300 ms we noticed a decrease in the intensity of the diagonal signal accompanied by the formation of clearly visible off-diagonal correlations between the individual components of the quadrupolar spectrum. This indicates magnetic inequivalence of the interacting MPBA molecules probably caused by their different orientations toward the direction of the external magnetic field. This suggestion, however, requires verification by the determination of a complete 3D crystal structure of crystalline (2-methylpropyl)boronic acid. XRPD measurements and structure refinements are currently under progress and will be included in our separate contribution dealing with detailed simulations of the 2D spectra.
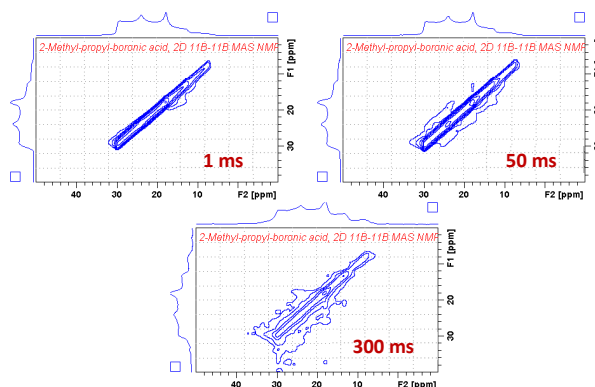

Figure S22. ^{11}B-^{11}B PDSD NMR correlation spectra (2-methylpropyl)boronic acid measured with ^{11}B-^{11}B spin-diffusion mixing times of 1, 50 and 300 ms.

2D ^{11}B-^{11}B DQ/SQ BR2$^1_2$ MAS NMR: As expected, comparting with the crystalline boric acid the observed relatively slower build-up of ^{11}B DQ coherence shown in **Figure S23** reflects longer boron-boron interatomic distances between the neighboring molecules of (2-methylpropyl)boronic acid. It is clear that maximum intensity of DQ coherence is detected at 1800-2000 µs of the recoupling period (9-10 recoupling cycles), whereas using the 600 µs recoupling period only 16% of this intensity is reached. Applying the shorter recoupling periods (200 and 400 µs) then leads to the generation of artificial coherences. These artificial signals are particularly apparent in the 2D ^{11}B-^{11}B DQ/SQ BR2$^1_2$ MAS NMR spectrum measured with 1 recoupling cycle (**Figure S24**). At 400 µs the artificial signals are considerably suppressed, whereas the correct DQ coherences are substantially intensified.
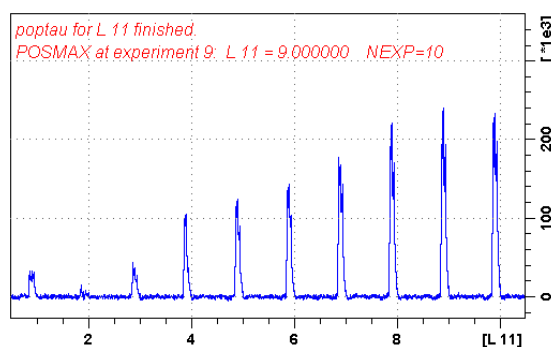

Figure S23. Optimization of ^{11}B-^{11}B DQ/SQ BR2$^1_2$ MAS NMR sequence using the crystalline (2-methylpropyl)boronic acid. Number of recoupling loops was optimized.
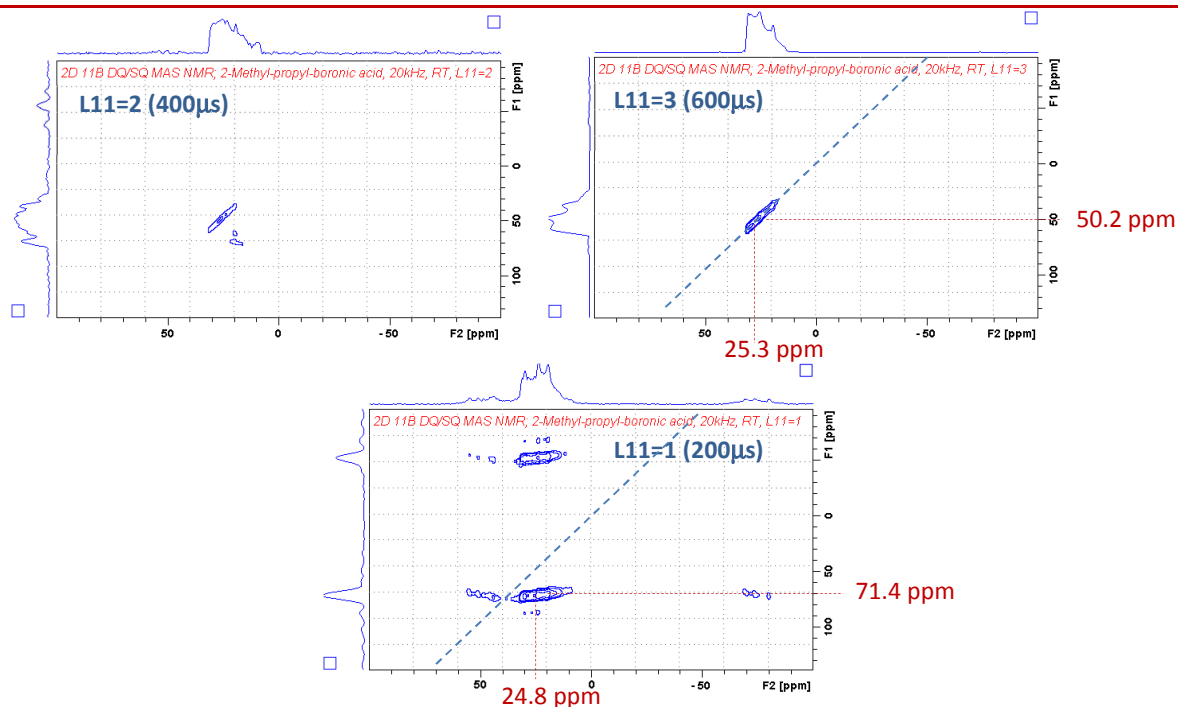
Figure S24. 2D ^{11}B-^{11}B DQ/SQ BR2$^1_2$ MAS NMR spectra of crystalline (2-methylpropyl)boronic acid measured at 200, 400 and 600 μs recoupling times.

***ad. v*) 2D ^{11}B-^{11}B experiments on [(E)-4-(2-Cyano-2-ethoxycarbonylvinyl)phenyl]boronic acid pinacol ester (C$_{18}$H$_{22}$BNO$_4$)**

A crystalline compound [(E)-4-(2-Cyano-2-ethoxy-carbonylvinyl)phenyl]boronic acid pinacol ester (CEPBA-PE, C$_{18}$H$_{22}$BNO$_4$, **Figure S25**) was used as the model molecular system in which boron atoms exclusively adopt trigonal coordination as clearly demonstrated by the isotropic chemical shift $\delta(^{11}$B) = 30 ppm and the second-order quadrupolar splitting being ca. 2.8 MHz. Because this boronic acid forms diester with pinacol the corresponding boron atoms cannot be involved in the covalent bonding with other molecules of boronic acid. In addition, the bulky substituents provide sufficient steric shielding to restrict formation of non-covalent boding between the boron sites too. Consequently, we suppose the extensive separation of boron atoms resulting in large boron-boron interatomic distances (>5 Å).
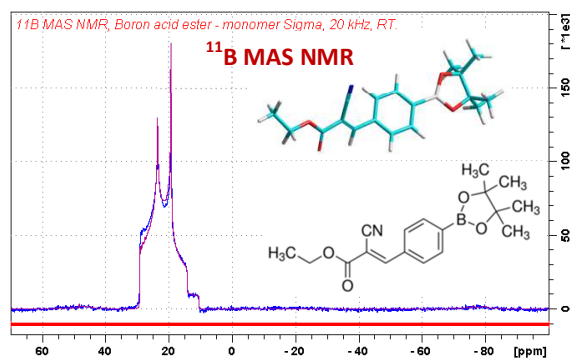
Figure S25. Chemical structure of CEPBA-PE and the corresponding ^{11}B MAS NMR spectrum with a line-shape simulation (isotropic chemical shift $\delta(^{11}$B) = 30 ppm; second-order quadrupolar splitting Q_{cc} = 2.8 MHz; asymmetry parameter of η=0.53).
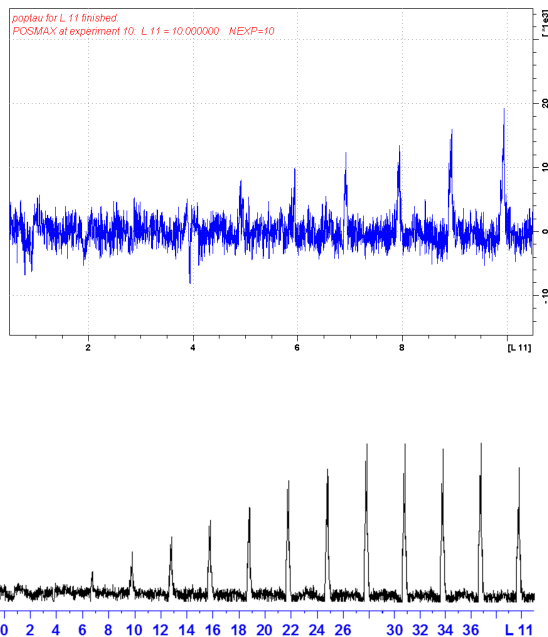
2D ^{11}B-^{11}B PDSD MAS NMR: In contrast to crystalline boric acid and 2-methylpropyl)boronic acid absolutely no magnetization transfer was observed in the standard NOESY-type 2D ^{11}B-^{11}B PDSD MAS NMR spectra (**Figure S26**). No off-diagonal signals appeared even using the mixing time reaching 500 ms. Moreover, no changes in the spectral pattern or loss of the coherence was observed. The intensity of the diagonal

signal remained unchanged, and no broadening toward the off-diagonal frequencies was observed. This finding thus strongly support our assumption that typical boron-boron interatomic distances in this CEPBA-PE system are considerable longer than that in crystalline (2-methylpropyl)boronic acid.
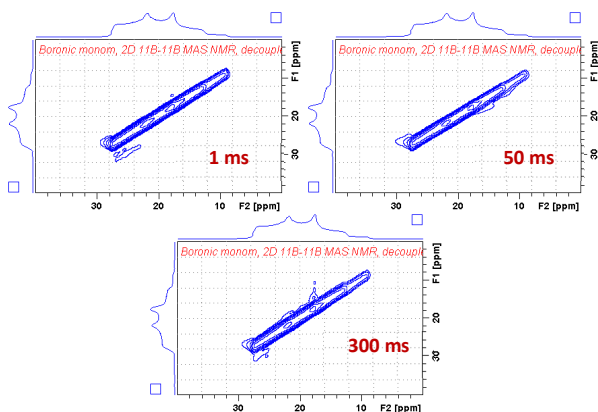

Figure S26. ^{11}B-^{11}B PDSD NMR correlation spectra of CEPBA-PE measured with ^{11}B-^{11}B spin-diffusion mixing times of 1, 50 and 300 ms.

Figure S27. Optimization of ^{11}B-^{11}B DQ/SQ BR2$^1_2$ MAS NMR sequence using the crystalline CEPBA-PE.

2D ^{11}B-^{11}B DQ/SQ BR2$^1_2$ MAS NMR: The above-indicated long-range boron-boron interatomic distances in the crystalline CEPBA-PE were subsequently confirmed by the observed very slow DQ coherence build-up and overall low efficiency of DQC excitation (**Figure S27**). No measurable DQ coherence was excited using the recoupling periods of 200-1000 μs. Moreover, the DQC buildup was not finished even using the recoupling time reaching 2000 μs (10 recoupling cycles). By repeating the optimization experiment the maximum intensity of ^{11}B DQ coherence was found at 5600-6000 μs of the recoupling period (28-30 recoupling cycles).

Consequently, due to the low efficacy in the ^{11}B DQC excitation the corresponding 2D ^{11}B-^{11}B DQ/SQ BR2$^1_2$ MAS NMR spectra of crystalline CEPBA-PE measured with short recoupling periods (200-600 μs) demonstrate only the intensive artificial signals (**Figure S28**). Correct and acceptably strong DQ ^{11}B-^{11}B signals were detected using the considerably longer recoupling times reaching more than 1000 μs. Although the intensities of DQ ^{11}B-^{11}B correlation signals detected for this compound are still relatively weak, in comparison with all the above discussed crystalline compounds, the ability to detect correlation coherences for the long-range spin pairs is generally very promising.

14
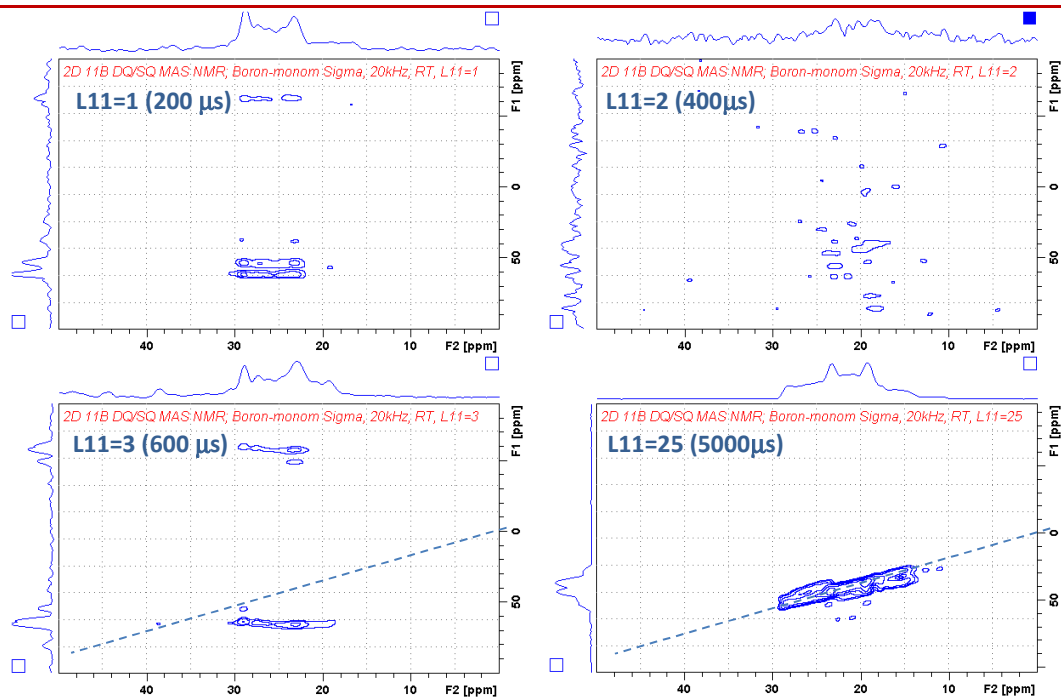
Figure S28. 2D ^{11}B-^{11}B DQ/SQ BR2$^1_2$ MAS NMR spectra of [(E)-4-(2-Cyano-2-ethoxycarbonylvinyl)phenyl]- boronic acid pinacol ester measured at 200, 400, 600 and 5000 µs recoupling times.

Supporting Information S3 – 2D ^{11}B-^{11}B Correlation Experiments on Bortezomib Polymorphs

2D ^{11}B-^{11}B TQ/MAS PDSD NMR: Due to the lack of resolution and sensitivity observed in the ^{11}B-^{11}B PDSD MAS NMR spectra of Bortezomib polymorphic Form I (see the main text) we alternatively applied 2D ^{11}B-^{11}B TQ/MAS PDSD NMR technique employing selection and evolution of the triple-quantum (TQ) coherence. This way, we were able resolve two trigonal boron sites B^{III}_3-B^{III}_2 (**Figure S29 up**). Moreover, applying the 100 ms mixing time we detected well-resolved correlation signals (**Figure S29 bottom**) confirming spatial proximity of B^{III} and B^{IV} species. However, the expected B^{III}_1-B^{III}_2 correlation still remained hidden.
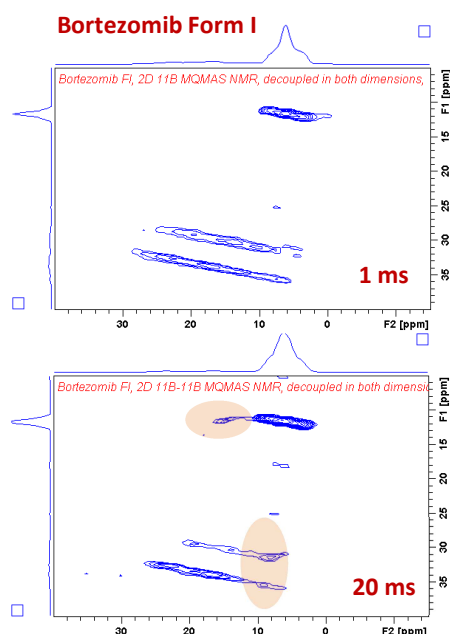
Bortezomib Form I


Figure S29. ^{11}B-^{11}B TQ/MAS PDSD NMR correlation spectra of Bortezomib polymorphic Form I measured with ^{11}B-^{11}B spin-diffusion mixing times 0, and 20 ms

2D ^{11}B-^{11}B DQ/SQ BR2$^1_2$ MAS NMR: As demonstrated in **Figure S30** the recorded DQ coherence buildups of both Bortezomib polymorphic forms go through the maxima reached at ca. 600-800 μs of the recoupling period.

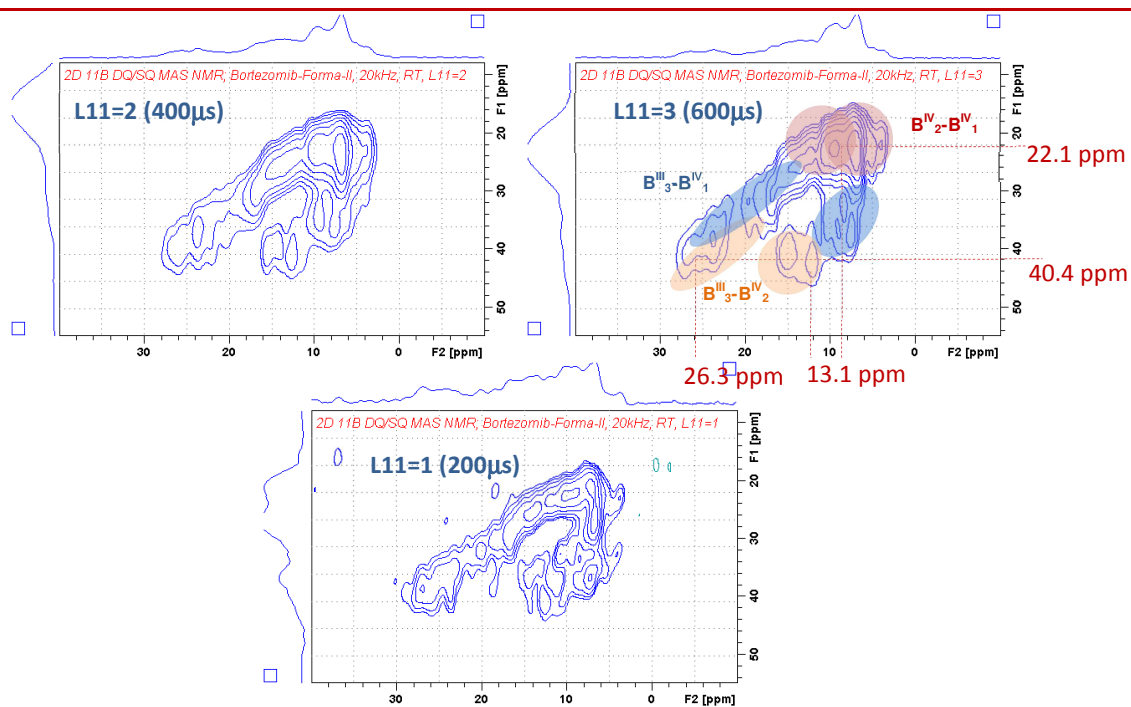**Bortezomib Form I**
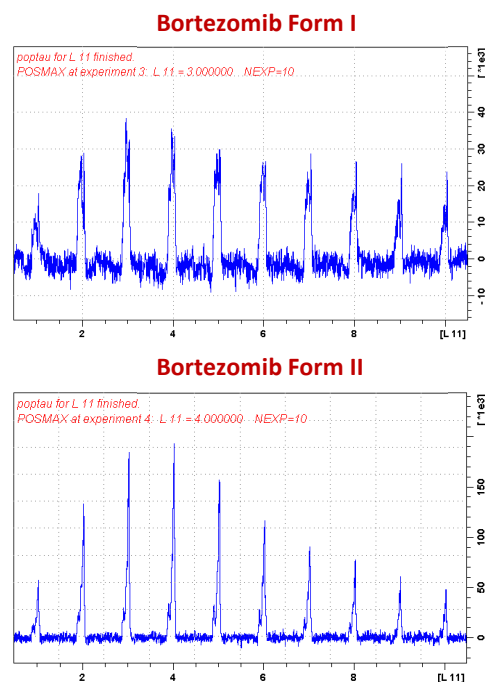
Bortezomib Form II

Figure S30. Optimization procedure of the ^{11}B-^{11}B DQ/SQ BR2$^1_2$ MAS NMR sequence using the crystalline Bortezomib polymorphs Form I and Form II. Number of recoupling loops was optimized and the length of a recoupling loop (synchronized with MAS frequency) was 200 μs.

The corresponding 2D ^{11}B-^{11}B DQ/SQ BR2$^1_2$ MAS NMR spectra recorded at 200, 400 and 600 μs recoupling times are demonstrated in **Figures S31** and **S32**. From these spectra it is clear that correlation signals appear at the expected DQ-SQ frequency regions even at 200μs, while no artificial signal can be detected. This finding definitely confirms short B-B distances in the investigated systems.
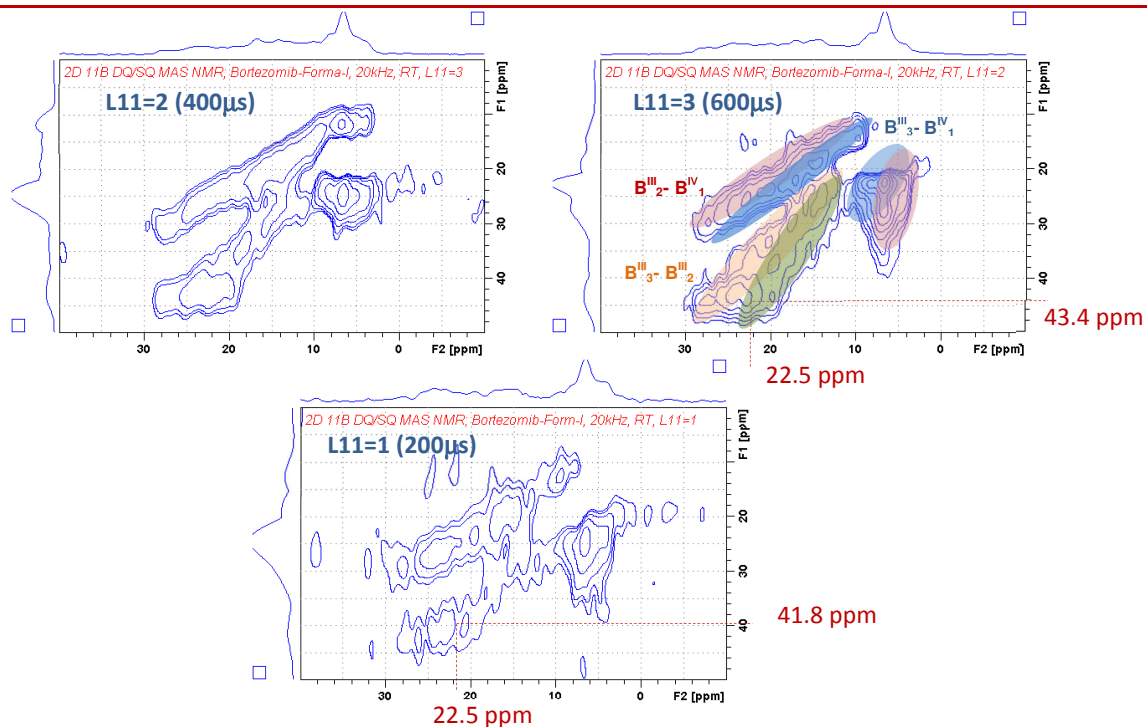
**Figure S31**. 2D ^{11}B-^{11}B DQ/SQ MAS NMR spectra of Bortezomib Form I measured at 200, 400 and 600 μs recoupling times.

Figure S32. 2D ^{11}B-^{11}B DQ/SQ MAS NMR spectra of Bortezomib Form II measured at 200, 400 and 600 μs recoupling times.

Analysis of ¹H-¹³C FSLG HETCOR spectra demonstrated in **Figures S33** and **S34** is strongly complicated by the existence of the three structurally and magnetically non-equivalent bortezomib fragments or molecules in the investigated polymorphic Forms I and II. This fact leads to a triplicate number of the correlation signals. Therefore, some parts of the obtained spectra are overcrowded by the correlation resonances and complete signal assignment without the aid of isotopic labeling allowing for measurements ¹³C-¹³C INADEQUATE experiments is nearly impossible. Moreover, the skeleton of Bortezomib molecule contains 4 nitrogen atoms that further complicate tracing the long-range ¹H-¹³C connectivity. Nevertheless, by combining the ¹³C CPPI/MAS NMR experiment discriminating CH_3, CH_2, CH and C carbon units (red traces in **Figures S33** and **S34**) with DFT computations of isotropic chemical shifts we were able to assign the resonances of the key parts of bortezomib molecules. Specifically, we focused on the carbonyl carbons CO no. 6 and 15, and CH unit no. 7.
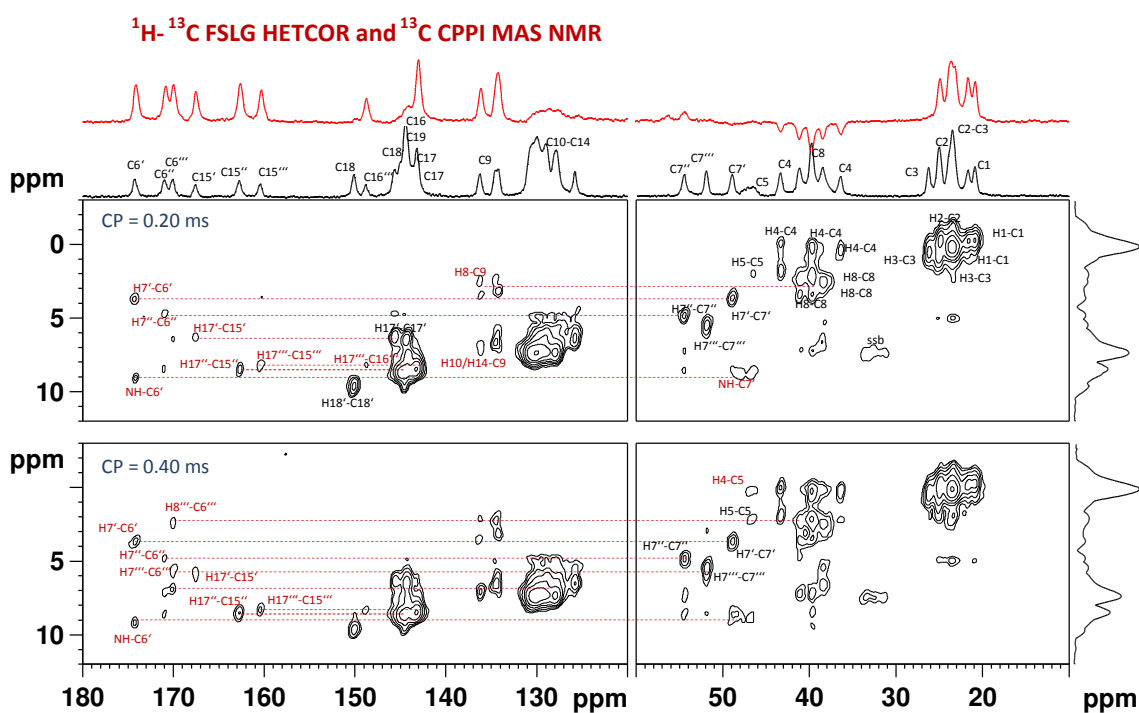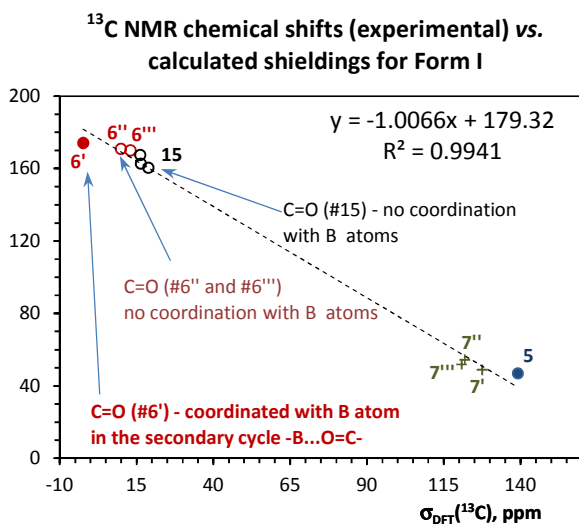

Figure S33. 2D ¹H-¹³C FSLG HETCOR NMR spectra of crystalline Bortezomib Form I measured at 200, and 400 μs cross-polarization mixing times.

^{1}H-^{13}C FSLG HETCOR and ^{13}C CPPI MAS NMR
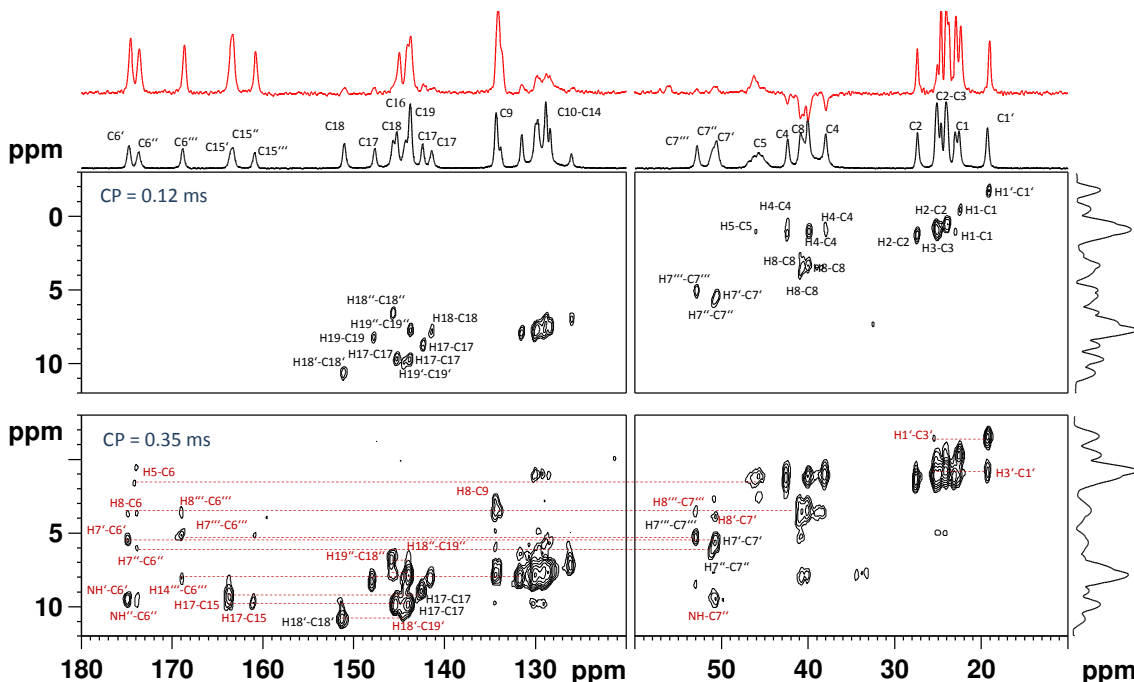
Figure S34. 2D ^{1}H-^{13}C FSLG HETCOR NMR spectra of crystalline Bortezomib Form II measured at 120, and 350 μs cross-polarization mixing times.

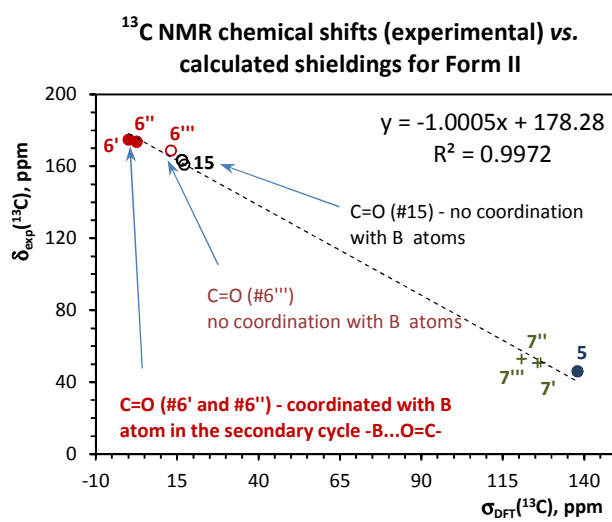**Figure S35.** ^{13}C NMR isotropic chemical shifts (experimentally determined) and their corresponding isotropic chemical shieldings as calculated by the GIAO-B3LYP/6-311G** approach for bortezomib Form I.
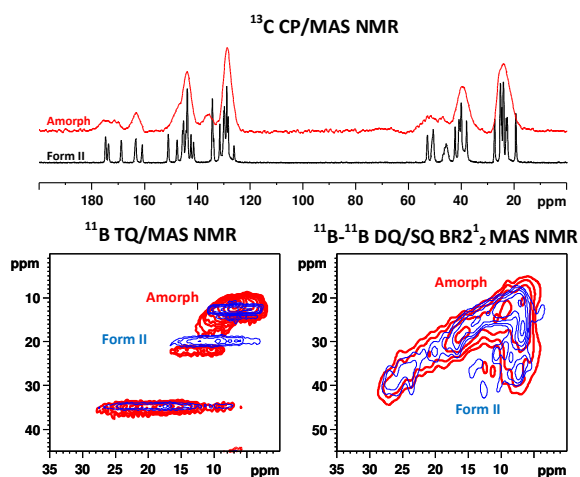
Figure S36. ^{13}C NMR isotropic chemical shifts (experimentally determined) and their corresponding isotropic chemical shieldings as calculated by the GIAO-B3LYP/6-311G** approach for bortezomib Form II.

Figure S37. Overlay of ^{13}C CP/MAS NMR, ^{11}B TQ/MAS NMR and $^{11}BDQ/SQ$ $BR2^1_2$ MAS NMR spectra of amorphous form (red lines) and polymorphic Form II (blue lines) of bortezomib.

Supporting Information S6 –Electron Diffraction Analysis

Boroxine structure of bortezomib Form II was preliminary studied by electron diffraction in cooperation with the University of Mainz. Although it is still impossible to refine complete 3D structure the determined volume of the symmetry independent part of bortezomib Form II corresponds nearly exactly to one boroxine structural motif. Moreover, the presence of three symmetry independent molecules of boronic acid in the symmetry independent part would be very unlikely from the crystallographic point of view. The resulting possible space groups are: P21/n (14), P212121 (19), Pca21 (29), Pna21 (33), and the Pawley refinement of the electron powder diffraction pattern for the P212121 space group (Form II), reveled the unit cell parameters a= 31.19 Å, b = 17.84 Å, c = 10.99 Å, and $\alpha = \beta = \gamma = 90^o$. Consequently, the calculated volume of this orthorhombic unit $P2_12_12_1$ is a.b.c = 6115 $Å^3$, and the volume of symmetry independent part (Z = 4) being 1529 $Å^3$ well corresponds to the estimated volume for 3 bortezomib molecules in the boroxine form ((57+3+12+9) x 15 + 69 x 5 = 1560 $Å^3$).

Conversely, assuming 3 bortezomib molecules in the free acid form the estimated volume of symmetry independent part is larger being ca. 28 x 15 + 25 x 5 = 1635 $Å^3$.

Because the crystal structures of bortezomib polymorphs are still unknown we generated/predicted a set of possible candidates using a program package Polymorph Predictor (Materials Studio). As an initial input model structure we used the previously DFT optimized boroxine cycles. The resulting predicted results showing the crystal lattice parameters similar to the parameters obtained by the analysis of electron diffraction data were subsequently used to the DFT geometry optimization. The currently most consistent prediction of the crystal structure of bortezomib showing boron atoms in B^{III} and B^{IV} local geometry demonstrated in **Figure S36** exhibits the following lattice parameters: a= 27.94 Å, b =19.44 Å, c = 11.55 Å, $\alpha = \beta = \gamma = 90^o$ for $P2_12_12_1$ space group.
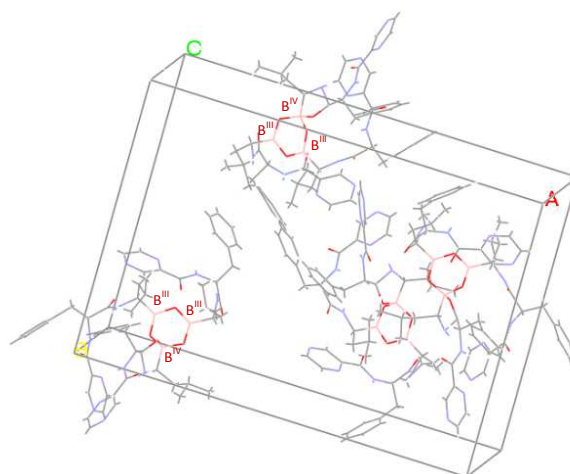
Figure S38. Predicted crystal structure of crystalline Bortezomib (Polymorph Predictor, Materials Studio).

It is worthy to note, that the difference between the experimentally estimated cell volume (6115 Å) from electron diffraction analysis and the predicted value (6273 Å) is less than 2.5%. Moreover, the optimized structure adopts both possible local co-ordinations of boron atoms (B^{III} and B^{IV}) in boroxine cycle as expected. Consequently, we believe that the presented structure correctly represents one of bortezomib's polymorphs. However, much more DFT optimizations and computations NMR parameters must be done to verify this assumption and to refine complete 3D crystal structures for both polymorphic forms of bortezomib. This work is currently under progress.

References

1. Gainsford, Graeme J.; Kemmitt, Tim; Higham, Caleb, *Acta Crystallographica Section E*, **2008**, 5, i24-i25/
2. Zalkin, A.; Hopkins, T.E.; Templeton, D.H. *Inorg. Chem.* **1967**, *6*, 1911.
3. Gajhede, M.; Larsen, S.; Rettrup S. *Acta Crystallographica, Section B* **1986**, *42*, 545-552.
4. Eden, M.; Frydman, L. J. Phys. Chem. B **2003**, *107*, 14598-14611